J Mater Sci (2009) 44:1113–1120
DOI 10.1007/s10853-008-3161-5

Reinforcement of SC-15 epoxy with CNT/CNF under high magnetic field: an investigation of mechanical and thermal response

Hassan Mahfuz · Shaik Zainuddin · Martin R. Parker · Tariq Al-Saadi · Vijay K. Rangari · Shaik Jeelani

Received: 18 June 2008 / Accepted: 5 December 2008 / Published online: 22 January 2009

Abstract We report here reinforcement of SC-15 epoxy matrix with 1.0 wt% loading of carbon nanotubes (CNTs)/carbon nanofibers (CNFs), and cured under a high (28 T) magnetic field. The improvement in mechanical properties such as compressive strength and stiffness was phenomenal with CNT inclusion, about 126% and 166% increase in strength and modulus, respectively. Enhancement in the glass transition (T_g) and thermal decomposition temperatures was also significant, by about 30 and 23 °C, respectively. Although the degree of anisotropy introduced by the magnetic field was not significant, it was observed that almost half of the improvement was due to magnetic flocculation. In the following is described the results of initial experiments conducted in the National High Magnetic Field Laboratory (NHMFL). Enhanced properties of the nanocomposites strongly suggest improved ordering of nanoparticles within the matrix.

Introduction

Extensive studies [1–4] have been carried out over the last several years on the detection of changes in a wide range of physical characteristics of polymers subjected to high magnetic fields during the curing stages. The enhancement of mechanical and thermal properties of pure polymer matrices by the addition of small volume fraction of nanoparticles (NPs) is also well documented [5, 6]. These gains in physical attributes by the formation of nanocomposites (NCs) have also been achieved using conventional processing techniques with no apparent changes in terms of appearance, density, and aging. Nanocomposites are now under consideration for major application in the packaging, coating, electronic, automotive, and aerospace industries [7].

Elongated (carbon) nanofibers and nanotubes, with their high aspect ratios, have been particularly attractive in this area of investigation, given that the load transfer mechanisms at the interface between the NPs and matrix are crucially important. The bulk mechanical strength and stiffness of such composites is directly dependent on this interface. The elongated cylindrical forms of both multi-walled carbon nanotubes (CNTs) and carbon nanofibers (CNFs) result in anomalously large interface area per particle. CNTs with their elastic modulus in the TPa range and strength of several hundred GPa have recently become excellent reinforcing materials for various matrices [8–11]. On the other hand, the advent of vapor-grown carbon fibers, with transverse dimensions in the nanometer range and with relatively lower production costs has added considerable interest and effort to this area of study.

Understandably, much of the recent effort in this field has focused on the development of suitable techniques for the alignment of these nanofibers and nanotubes along preferred directions. One popular approach has been that of mechanical extrusion, including recent efforts by some of the present authors to extrude hot melts of linear low-density polyethylene powder and carbon nanowhiskers through small dyes [12]. As the nanotubes and nanofibers are highly

H. Mahfuz (✉)
Florida Atlantic University, Boca Raton, FL 33431, USA
e-mail: hmahfuz@oe.fau.edu

S. Zainuddin · V. K. Rangari · S. Jeelani
Tuskegee University's Center for Advanced Materials (T-CAM), Tuskegee, AL 36088, USA

M. R. Parker · T. Al-Saadi
Department of Electrical and Computer Engineering, University of South Alabama, Mobile, AL 36688, USA

entangled in the polymer, it would require a large moment exerted by the magnetic field for a considerable period of time to cause any rotation and subsequent alignment of acicular particles. The topic has been covered in [13].

In the following, we describe efforts to align CNTs and CNFs in a single preferred direction in bulk polymer matrices by the application of magnetic fields during the curing process.

Theory

There is, to our knowledge, no published theoretical model for the behavior of CNTs and CNFs in high uniform magnetic fields and no serious attempt is made here to change that situation. One simple explanation for the lack of a model is the extreme complexity of the problem predicated on the fact that these (highly acicular) particles are not rigid nanocylinders. They are, moreover, susceptible to entanglement with other particles through powerful Van der Waals interactions and are of such extreme acicularity, (500–1000, for example), that the normal dipolar particle behavior in a high uniform field is essentially lost. That notwithstanding, a modest understanding of what happens to these NPs in high magnetic fields may be gained by ignoring, in the interests of simplicity, the lack of particle rigidity as well as the other complications mentioned above.

The anisotropy of the axial and radial components of the magnetic susceptibility in acicular carbon NPs is well documented [14, 15]. Unfortunately, there is a lack of agreement within the scientific community as to whether the radial or the axial component of the magnetic volume susceptibility is the larger [16]. If a (rigid) acicular particle of this type is tilted in an arbitrary direction with respect to an applied uniform magnetic field within a fluid matrix, the NP is subjected to two competing torques (Fig. 1). Since the NP is diamagnetic, the induced radial (m_1) and axial (m_2) moments are negative. If the radial susceptibility is *larger* than its axial counterpart, a rigid NP will ultimately rotate into alignment with the magnetic field axis (Fig. 1) (Note that we have made this assumption in the experiments described in the following section). This susceptibility is extremely small in absolute terms, which means that enormous magnetic fields are required to exert sufficient torque to overcome Brownian motion and to orient sufficient numbers of these NPs along the field direction. Further, severe time constraints are placed on the whole exercise. The rate at which the NP processes is determined by the magnitude of the net torque (i.e., by the magnitude of the magnetic field) and by the viscosity of the matrix. The precession must be completed during the curing process and, in particular, during the pre-gel stage at which time the viscosity of the matrix is still relatively modest.

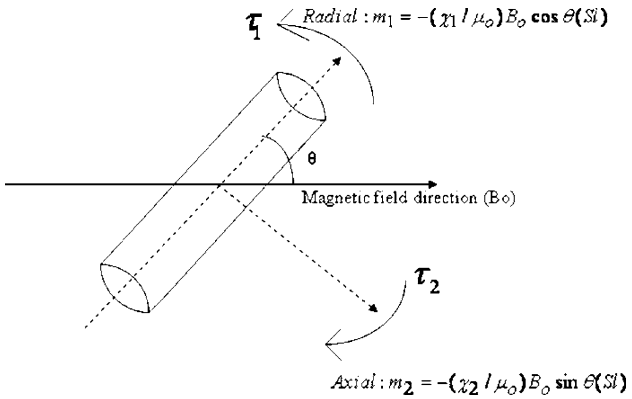

Fig. 1 Schematic of a rigid acicular nanoparticle subjected to competing torques in a uniform applied magnetic field

A further mechanism must be introduced to describe what happens at higher values of applied magnetic field. The mechanism in question, magnetic flocculation [17, 18], is a well-known one in which small particles, through the mutual attraction of magnetic dipoles induced on each of them by the external magnetic field, agglomerate in pairs, or higher number groups, in linear fashion along the field direction. Even this well-known phenomenon, however, is complicated by the extreme acicularity of the NPs investigated here, in that, in the presence of a magnetic field, the two end tips of a single NP are so far removed from one another that the dipolar characteristics are essentially lost and, to all intents and purposes, single poles at the NP tips attract others of opposite polarity on adjacent particles. Even so, the end result is much the same, with NPs having a tendency to join head-to-tail but in a fashion defying simple modeling.

Experiments

The preparation of the NCs was undertaken in two separate stages. First, acicular NPs were added at a 1% loading, by weight, to part A of SC-15 epoxy resin (60–70% diglycidylether of bisphenol A, 10–20% aliphatic diglyciylether, and 10–20% epoxy toughener) and dispersed by acoustic cavitation. Two specific types of acicular NPs, (CNTs and CNFs), have been considered. The MWCNTs used in our study were obtained from MER Corporation (7960 South Kolb Road, Tucson, AZ 85706, USA). The nanotubes were 5–15 nm in diameter, and approximately 5 μm long, with 5–20 graphitic layers. The remainder of the deposit was multi-layer polygonal carbon nanoparticles and amorphous and graphitic carbon nanoparticles. On the other hand, CNFs used in this work were type Pyrograf-III, PR–19 (Pyrograph Products Inc., 141 Xenia Ave, Cedarville, OH 45314, USA) having diameter of 100–200 nm and length of 30–100 μm. The dispersion was carried out in a Sonic

Vibra Cell Ultrasound liquid processor for about 30 min at room temperature. The vessel containing the composite was externally cooled during this process to prevent undesired temperature rises. Following infusion of the nanoparticles, the modified epoxy part A was mixed with part B (hardener), comprising 70–90% of cycloaliphatic amine and 10–30% of polyoxylalkylamine. The hardener was added to part A at a volume ratio of 3:10. Mixing was promoted with a high-speed mechanical stirrer for about 5 min. The mixture was then vacuum-degassed for 10–15 min. After completion of this sample preparation step, the mixture was poured into cylindrical PVC tubes of a length and diameter designed to match the most uniform portion of a high-field Bitter magnet. The length and diameter of the cylinder was 203 mm by 25.4 mm, respectively. The experiments were conducted at the National High Magnetic Field Laboratory (NHMFL) located in Tallahassee, Florida. The tube was held co-axially inside the magnet using mechanical means. The curing of various samples took place within the magnet (28 T) for about 3 h. During this time, the resin gelled completely. Our previous experiments [19] with SC-15 have shown that at 3 h, the effect of magnetic fields actually leveled off. After 3 h, the tubes were taken outside the magnet and were allowed to cure at room temperature for 24 h. Once fully cured, cylindrical samples were dislodged from the tube and machined for mechanical and thermal tests.

Results and discussion

Static compression, dynamic mechanical analysis (DMA), and thermo-gravimetric analysis (TGA) tests were performed. Compression tests were performed on test coupons of dimension 12.5 × 12.5 × 25 mm^3, cut from the cylindrical samples. Four replicate test coupons of each sample were examined on a hydraulically controlled MTS machine to ASTM standards (D695-89). Dynamical mechanical analysis (DMA) tests were undertaken to determine the thermal transition temperature and the elastic response as a function of temperature. Thermo-gravimetric analyses were also carried out on all categories of samples to detect any magnetic-field induced changes in the thermal stability of the composites.

Quasi-static compression tests

Compression test data in tabular form is shown in Table 1. Nanocomposites reinforced with CNF showed strength and stiffness increase, respectively, by 40% and 55% compared to the neat epoxy control system. On the other hand, when the reinforcement was CNTs, the improvement was 126% and 166%, respectively. Typical stress–strain diagrams for CNF and CNT systems are shown in Fig. 2. It is clearly demonstrated that in both cases there is enhancement in both strength and modulus of the composite with the addition of nanoscale reinforcement and it is further

Table 1 Compressive properties of nanocomposites in the field direction (magnetic strength, 28 T)

Material	Magnetic curing time (h)	Compressive strength (MPa)	Gain/loss in strength (%)	Compressive modulus (GPa)	Gain/loss in modulus (%)
Neat SC-15	0	58.5 ± 1.4	–	1.50 ± 0.13	–
Neat SC-15	3	70.5 ± 2.0	+20	2.20 ± 0.24	+47
1% CNF	0	68 ± 2.4	+16.7	2.19 ± 0.17	+50
1% CNF	3	82 ± 2.5	+39.6	2.26 ± 0.17	+55
1% CNT	0	98 ± 2.4	+67	2.69 ± 0.2	+84
1% CNT	3	132 ± 3.2	+126	3.89 ± 0.12	+166

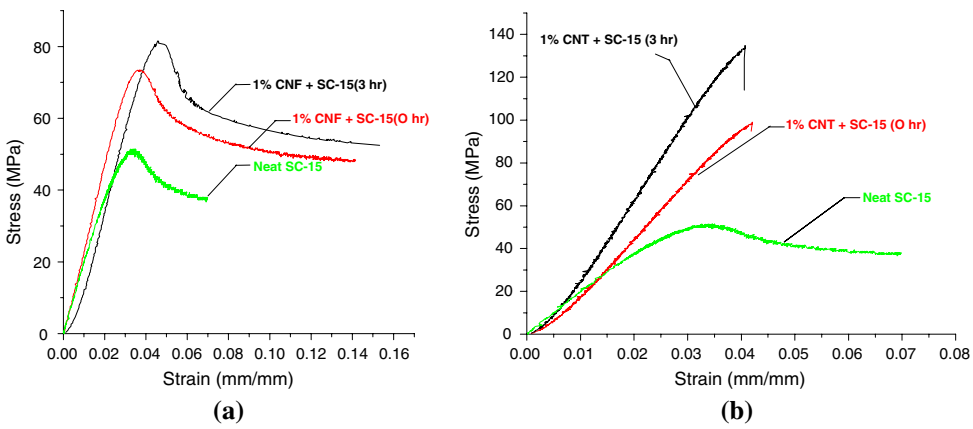

Fig. 2 Compressive response of **a** 1 wt% CNF and **b** 1 wt% CNT nanocomposites, cured for 0–3 h in a 28 T field. Also shown a comparison with neat samples cured under no magnetic field (0 h)

enhanced by the application of magnetic field. Huge improvement in strength and stiffness is obvious from the fact if CNTs are aligned along the specimen axis, they will share a large portion of the axial compressive load. Since the modulus of CNTs is significantly higher, load carried by CNTs will accordingly be higher. This load sharing would also depend on the strength of the interface between CNT and the matrix. Since the interface between CNT and polymer was strong, we saw a large increase in strength. On the other hand, the modulus of the NC was directly related to the alignment and the modulus of the reinforcement. It is also noticed in Fig. 2 that the gain in strength and modulus is also accompanied by gain in ultimate fracture strain, especially in case of CNF reinforcement. Fracture strain was calculated from the stress–strain diagram as shown in Fig. 2. It is seen in Fig. 2a that fracture strain for 1 wt% CNF with 3-h magnetic flocculation, has increased from 7% to 16%. Since the machine was run under load control, we believe the ultimate fracture point after prolonged plastic deformation represents the true fracture strain. It is, however, slightly different with the CNT system. In this case (CNT), there is a modest loss in fracture strain, but it is still within 4%.

Table 1 also reveals that if neat polymer is simply cured in an uniform magnetic field, its strength and stiffness increase by 20% and 47%, respectively. Similar behavior was also reported earlier [19]. Experiments have shown that epoxy resin behaves like a liquid crystalline system with respect to a magnetic effect [20]. Since the chemical groups in the molecule of the oligomer and curing agent have different magnetic permeability, the behavior of a molecule in a magnetic field can differ from the behavior of a rigid diamagnetic rod. As a result, the crystals formed will be of a nonequilibrium dissipative character. This will in turn affect the course of the curing reaction. It is also reported that the magnetic field will cause an increase in the number of hydrogen bonds as well as intermolecular C–O–C bonds in the epoxy resin under the effect of a magnetic field. These are the reasons that a magnetic field will control polymer properties.

It is known that infusion of nanoparticles itself enhances the polymer properties which is also seen to be true in this case. It is further enhanced by subjecting the polymer to cure under the magnetic field when the viscosity of the polymer is relatively modest. In making a comparison between the flocculated and nonflocculated systems, i.e., with 0 and 3 h magnetic curing time, it is observed that at least half of the improvement in properties has been contributed by magnetic flocculation. It gives a clear indication that properties of polymers can be significantly enhanced by curing the polymers at high magnetic field for a length of time (3 h) until the resin had completely gelled. Comparing the improvement in strength and modulus, it is apparent that under identical conditions, CNTs are better reinforcing materials than CNFs, especially for epoxy matrix.

Dynamic mechanical analysis

Tests were also carried out under DMA to determine the storage modulus of these NCs by subjecting the test coupons to flexural loading. Figure 3a and b shows variation of storage modulii and tan δ, respectively for CNT reinforced composites. An increase in the storage modulus by about 1000 MPa and an increase of 30 °C in glass transition temperature are observed. It was also seen that a significant enhancement in mechanical stiffness and glass transition temperature (approximately 350 MPa and 30 °C) also occurs with the CNF reinforced composites similarly treated. In both cases, storage modulii decrease as they approach their glass transition temperature. The main area of concern is the temperature at which the storage modulus started decreasing. This temperature can be taken as the onset of glass transition. Here we notice that for the neat controlled system, the storage modulus starts dropping at a lower temperature when compared with the corresponding magnetically cured samples. It is also noticed in Fig. 3b

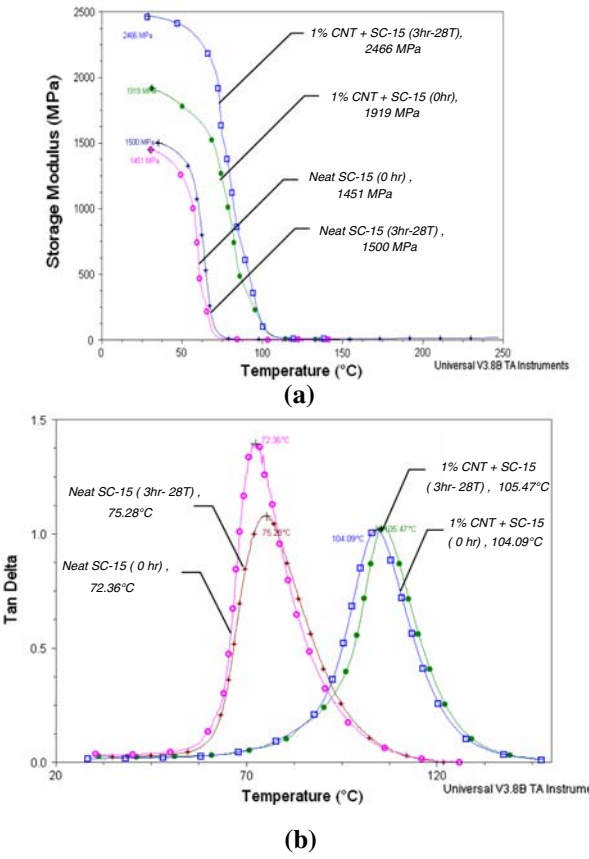

Fig. 3 **a**, **b** Storage modulus and glass transition temperature of nanocomposites

that there is a significant right shift in tan δ peak for the magnetically cured samples causing an enhancement in T_g.

Thermo-gravimetric analysis

Thermo-gravimetric analysis was carried out for the neat matrix and NCs to determine the effect of magnetic field on the thermal stability beyond glass transition and melting temperatures of the matrix. TGA monitors the weight loss as a function of temperature as the sample is heated to about 1000 °C range in an inert atmosphere. A typical TGA curve for neat epoxy sample is shown in Fig. 4a. As the polymer begins to decompose, weight loss becomes more and more prominent and at some point rate of weight loss is highest. This point is usually the peak of the derivative curve (DTG). In most cases of polymeric composites [21–23], DTG coincides with the 50% weight loss point as shown in Fig. 4a. Traditionally, this point is termed as the thermal decomposition temperature of the sample. Although the thermal decomposition temperature of the sample is well beyond the melting point of the polymer, it still bears the signature of polymer conformity before such decomposition. This is evident in Fig. 4b and c which show the decomposition behavior of SC-15 reinforced with 1 wt% CNT and CNF, respectively, without any magnetic flocculation. A comparison between Fig. 4a–c suggests that CNTs are better reinforcing materials than CNF for thermal stability as it was the case with mechanical properties. The decomposition temperature has increased from 375 to 386 °C with CNT, where as the increase is nominal

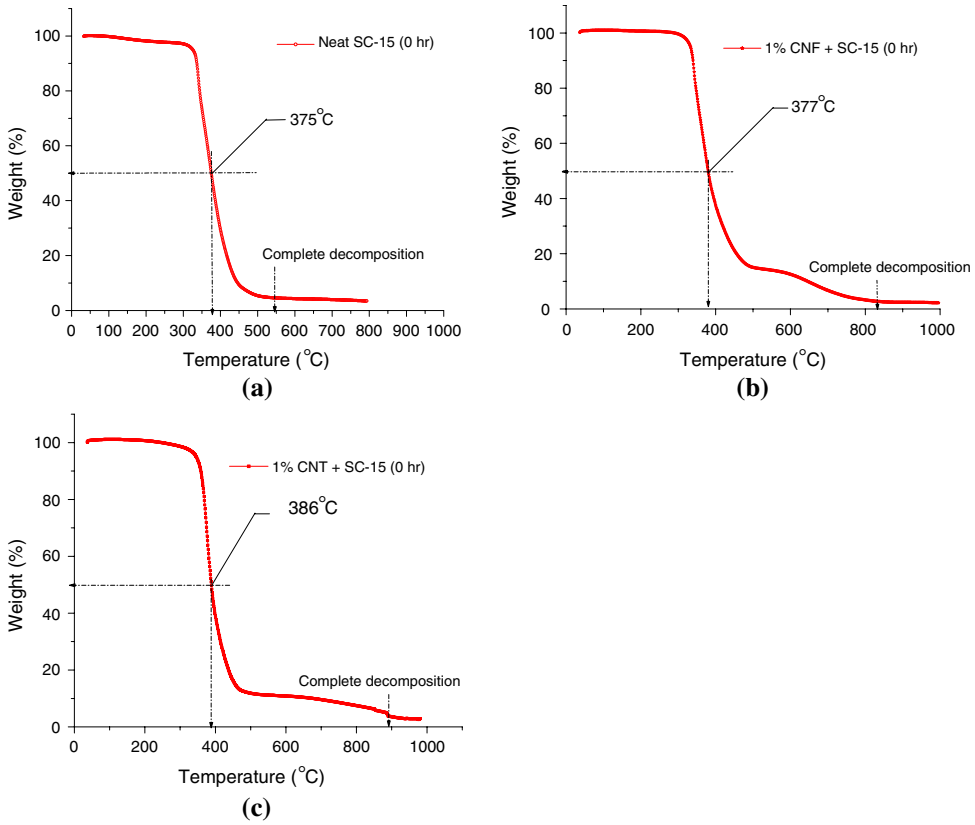

Fig. 4 **a–c** TGA curves of control (neat SC-15) and nanocomposites samples under no magnetic field (0 h)

Table 2 Thermal decomposition temperatures of various nanocomposites

Materials system	Magnetic field cure time (h)	Applied magnetic field strength (T)	Thermal decomposition temperature (°C)	Complete decomposition temperature (°C)
Neat SC-15	0	–	375 ± 1.04	550 ± 3.5
Neat SC-15	3		377 ± 1.16	720 ± 7.64
SC-15+ 1 wt% CNF	0	–	377 ± 1.52	840 ± 6.5
SC-15+ 1 wt% CNF	3	28	380 ± 1.5	890 ± 6.11
SC-15+ 1 wt% CNT	0	–	386 ± 1.76	891 ± 3.21
SC-15+ 1 wt% CNT	3	28	398 ± 2.03	920 ± 5.69

(377 °C) in case of CNF inclusion. Another decomposition feature can also be seen in Fig. 4a–c when the weight loss gets to the maximum or the TGA curve becomes horizontal. A comparison of the complete decomposition temperature shows (Table 2) that SC-15/CNT system has the highest value around 920 °C as opposed to 890 °C for SC-15/CNF composites under identical conditions. These thermal characteristics are consistent with the mechanical properties that we have discussed earlier.

Now if we look at the magnetically flocculated samples shown in Fig. 5a–c, the improvement in decomposition temperatures is clear. In case of CNF, the improvement is modest at 5 °C while it is 23 °C with CNT. In both cases, the samples were cured under 28 T for 3 h. An improvement of 23 °C is impressive and it exceeded 17 °C improvement that we observed earlier [19] with the inclusion of spherical TiO_2 nanoparticles. Another interesting feature is noticed in Fig. 5a–c that there exists somewhat weak second stage decomposition in each of the magnetically cured samples. This second stage decomposition is best visualized by DTG curves which are nothing but rate of weight loss as a function of temperature. The DTG curves are superimposed in Fig. 5a–c. As an example, if we look at Fig. 5c, it is seen that first-step decomposition occurs at around 360 °C range with a very sharp DTG peak at 350 °C indicating the initiation of a rapid and vigorous decomposition feature. The step is signaled by 7–10% weight loss and involves initial breakdown of the polymer backbone components. The first-step decomposition continues up to about 460 °C when the weight loss is around 85%. A second-stage decomposition characterized by a small and weak DTG is observed at 600 °C. This decomposition is due to extremely slow bleed of further 10–12% weight loss of the remaining polymer.

Compression tests perpendicular to the magnetic field

While it was obvious from mechanical and thermal analyses that reinforcement of CNFs and CNTs accompanied

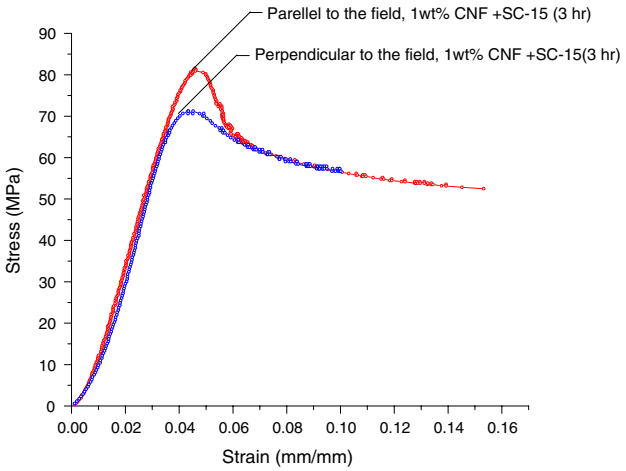

Fig. 6 Compression tests parallel and perpendicular to the field direction

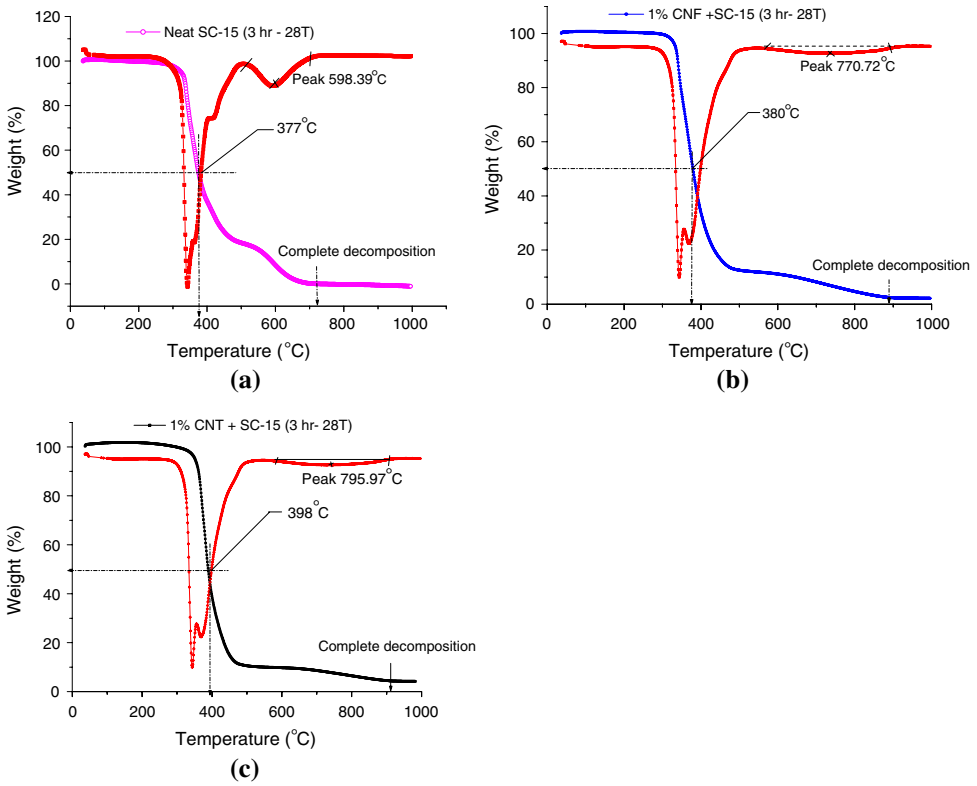

Fig. 5 **a–c** TGA and DTG curves of magnetically cured samples

Table 3 Compressive properties of nanocomposites tested parallel and perpendicular to the field direction

Material	Magnetic curing time (h)	Compressive strength (MPa)	Percent gain/loss in strength over perpendicular samples	Compressive modulus (GPa)	Percent gain/loss in modulus over perpendicular samples
1% CNF + SC-15 (perpendicular to field)	3	71 ± 1.4	–	2.21 ± 0.2	–
1% CNF + SC-15 (parallel to field)	3	82 ± 2.5	+15.5	2.26 ± 0.17	+2.3

by magnetic field curing brought significant improvement in properties, it is indeed important to show that such improvement in part was due to some preferred orientation of the nanoscale reinforcements. Without any chemical treatment of CNF/CNTs [24], we did not expect much of an alignment; however, any SEM micrographs of the type shown in the reference [19] would have been helpful. In absence of such micrographs, compression tests were performed by cutting samples parallel and perpendicular to the magnetic field. Representative stress–strain diagrams of SC-15/CNF samples for compression tests in the perpendicular direction are shown in Fig. 6. It is observed that the strength for parallel sample is about 15% higher than that of the perpendicular sample. In case of modulus, the difference is, however, nominal at 2.3% as shown in Table 3. This shows that some degree of anisotropy has been introduced due to magnetic flocculation. In both cases, strength and modulus are much higher than that of the neat samples as shown earlier in Table 1. It is to note that all data shown in Table 1 were collected from samples cut parallel to the field direction.

Conclusion

It has been observed that the mechanical and thermal properties of a polymer can be significantly improved by reinforcing it with acicular nanoparticles such as CNT/CNF and curing it under a strong magnetic field. The improvement in strength and modulus was 126% and 166%, respectively, with CNT and under 28 T magnetic field. However, enhancement with CNF inclusion was relatively lower, but still remained between 40% and 55% range. Enhancement in T_g and thermal decomposition temperature was also significant. For example, with SC-15/CNT (28 T) composites, the increase was by 30 and 23 °C, respectively. It is demonstrated through TGA experiments that when epoxy is reinforced with CNT/CNF and also subjected to magnetic field curing, NCs undergo a gradual (slow) loss of polymer as opposed to a rigorous loss observed in absence of the magnetic field. This causes a large increase in the final decomposition temperature. It was noticed that half of these improvements both in mechanical and thermal properties were brought about by magnetic flocculation. It is also shown that magnetic flocculation does introduce relatively modest anisotropy in the system, and mechanical properties are seen to be higher in the direction parallel to the field.

Acknowledgement A portion of this work was performed at the National High Magnetic Field Laboratory (NHMFL) which was supported by NSF Cooperative Agreement No. DMR-0084173, by the State of Florida, and by the DOE. We also acknowledge with appreciation the support for this work by ONR.

References

1. Barclay GG, Ober CK, Papathomas KI, Wang DW (1992) Macromolecules 25:2947
2. Barclay GG, McNamee SG, Ober CK, Papathomas KI, Wang DW (1992) J Polym Sci A Polym Chem 30:1845
3. Ober CK, Barclay GG (1991) Mater Res Soc Symp Proc 227:281
4. Lincoln MD, Douglas EP (1999) Polym Eng Sci 39:1903
5. Reynaud E, Gautier C, Perez J (1999) Rev Metall 96:169
6. Chun LW, Ming QZ, Min ZR, Klaus F (2002) Comp Sci Tech 62:1327
7. Mahfuz H, Islam M, Rangari V, Saha M, Jeelani S (2004) Compos B 35:543
8. Mahfuz H, Adnan A, Rangari VK, Hasan MM, Jeelani S, Wright WJ, De Teresa SJ (2006) Appl Phys Lett 88:083119
9. Camponeschi E, Vance R, Al-Haik M, Garmestani H, Tannenbaum R (2007) Carbon 45:2037
10. Treacy MMJ, Ebbesen TW, Gibsoj JM (1996) Nature 381:6584
11. Yu MF, Lourie O, Dyer MJ, Noloni K, Kelly TF, Ruoff RS (2000) Science 287:637
12. Mahfuz H, Rangari V, Adnan A, Jeelani S (2004) Compos A Appl Sci Manuf 35:519
13. Parker MR, Al-Saadi T, Mahfuz H, Zainuddin S, Rangari V, Jeelani S (2005) In: The 2nd international conference on nanocomposites and nanotechnologies (NN 2005), Crete, Greece, June 14–18
14. Wang XK, Chang RPH, Patashinski A, Ketterson JB (1994) J Mater Res 9:1578
15. Byszewski P, Baran M (1995) Europhys Lett 31:363
16. Tsui F, Jin L, Zhou O (2000) Appl Phys Lett 76:145
17. Svoboda J (1981) Int J Miner Process 8:377
18. Parker MR, Van Kleef RPAR, Myron HW, Wyder P (1982) J Mag Mag Mater 27:250
19. Mahfuz H, Zainuddin S, Parker MR, Al-Saadi T, Rangari VK, Jeelani S (2007) Mater Lett 61:2535
20. Rodin YP, Molchanov YM (1988) Effect of conformal changes caused by a homogeneous static magnetic field on curing of epoxy resin. Mech Compos Mater 24(3):380

21. Mahfuz H, Rangari V, Islam M, Jeelani S (2004) Compos A Appl Sci Manuf 35:453
22. Mahfuz H, Adnan A, Rangari V, Jeelani S (2005) Int J Nanosci (IJN) 4(1):55
23. Rodgers RM, Mahfuz H, Rangari VK, Chisholm N, Jeelani S (2005) Macromol Mater Eng 290(5):423
24. Shia D, He P, Lian J, Chaud X, Bud'ko SL, Beaugnon E, Wang LM, Ewing RC, Tournier R (2005) J Appl Phys 97:064312